Springer

Journal of
Mechanical
Science and
Technology

Journal of Mechanical Science and Technology 22 (2008) 387~396

www.springerlink.com/content/1738-494x

Evaluation of surrogate models for optimization of herringbone groove micromixer

Mubashshir Ahmad Ansari and Kwang-Yong Kim*

Department of Mechanical Engineering, Inha University, Incheon, 402-751, Rep. of Korea

(Manuscript Received April 4, 2007; Revised September 8, 2007; Accepted September 8, 2007)

Abstract

Surrogate models have been applied to shape optimizations of a micromixer with the aim of assessing the performance of the models. The surrogate models considered include polynomial response surface approximation, Kriging, and radial basis neural network. In addition, a weighted average model based on global error measures is constructed. A mixing index at the exit of the micromixer is used as the objective function. The mixing index is calculated based on Navier-Stokes equations. Two cases of optimization, one with two design variables and the other with three design variables, have been tested. The design variables are selected among the ratio of the groove depth to channel height, the angle of groove, and the ratio of groove width to groove pitch. D-Optimal design generated sampling points are used for sampling. It is found that although the weighted average model does not predict the best optimal point, it does show consistent and reliable performance.

Keywords: Shape optimization; Micromixer; Herringbone groove; Mixing; Surrogate model; Weighted average model

1. Introduction

Surrogate-based approximations are being increasingly used in single or multidisciplinary optimizations. Considering the competing requirements of computational economy, i.e., employing as few data points as possible for constructing a surrogate mode, and fidelity, i.e., offering high accuracy in representing the characteristics of the design space, the assessment of the performance of surrogate models is of critical importance.

Queipo et al. [1] and Li and Padula [2] reviewed various surrogate-based models used in aerospace applications. Zerpa et al. [3] presented a multiple surrogate model: a weighted average surrogate model based on response surface approximation (RSA), radial basis neural network (RBNN) and Kriging models. They determined weights for weighted average models considering pointwise estimation of variance for the three surrogate models. Goel et al. [4] also developed a global version of weighted average surrogate models using RSA, RBNN and Kriging models, where the weights are fixed and determined according to cross validation errors. The larger the error in prediction in any surrogate, the smaller the weight that is assigned. They concluded that the weighted average surrogate model is a more reliable prediction method than individual surrogates. Because the same training data can be repeatedly used, the cost of constructing multiple surrogates from the same simulation data is very small; it seems desirable to produce multiple optima to increase the likelihood of reaching the best outcome. Goel et al. [5] demonstrated the application of this approach to optimal model calibration in cryogenic cavitation.

Mixing of fluids in microdevices is a big challenge due to the predominantly laminar nature of the flow. Herringbone grooved micromixers proved to be good in enhancing mixing process. Stroock et al. [6]

*Corresponding author. Tel.: +82 32 872 3096, Fax.: +82 32 868 1716
E-mail address: kykim@inha.ac.kr
DOI 10.1007/s12206-007-1035-4

showed experimentally that mixing can be enhanced by using a repeating sequence of bas-relief herringbone-shaped asymmetric structures at an oblique angle on the floor of the channel. The main concept in this design is to create transverse flow patterns that increase the interfacial area between the fluids to be mixed. Shape optimization of the herringbone groove can be performed to enhance mixing.

Hessel et al. [7] reviewed the mixing principle of active and passive micromixers and also provided descriptions of typical designs of the mixing elements, characterization methods, and their applications. One of the passive methods to enhance the mixing process is the patterning of one or more surfaces of the channel by special shaped structures. In a simple microchannel (a channel without grooves or any other shape) with flow at low Reynolds number, the mixing of the fluids is purely diffusive, which is very slow or negligibly small as compared to convective mixing. The geometric parameter of the herringbone groove shape is found to be very effective in controlling the mixing of the fluids.

Stroock and McGraw [8] investigated analytically the effect of the asymmetry of the groove on mixing and reported a range for its optimum value. Aubin et al. [9] numerically investigated the effect of different geometrical parameters of a staggered herringbone groove micromixer on the mixing quality with the aim of improving the mixer design. A particle tracking method was used to visualize and quantify the mixing performance. They reported that the mixing quality is strongly influenced by small modifications in the geometry of the grooves. Hassell and Zimmerman [10] studied the effect of groove depth and Reynolds number on the flow characteristics to understand the mechanism of mixing for three different arrangements of the groove. The flow field within the groove at various heights and its relationship with the non-axial flow within the bulk channel was analyzed.

It is clear that mixing can be effectively increased by optimizing the shape of the grooves. As discussed above, some investigations have been carried out on the effects of geometric parameters on the mixing performance. However, systematic numerical optimization techniques [11] have not yet been applied to the micromixer geometries.

In the present work, surrogate models have been applied with the aim of accessing the performance of the surrogates along with shape optimization of a herringbone groove micromixer using Navier-Stokes equation to enhance mixing. The surrogates considered are RSA, RBNN, Kriging and a weighted average surrogate model. Three design variables, namely the ratio of depth of groove to height of channel, angle of groove, and the ratio of depth of groove to the pitch of groove, are selected as the design variables. D-optimal method is used to select the design points in the design space.

2. Problem description and numerical procedure

2.1 Micromixer model

Fig. 1 shows the geometry of the mixer with herringbone grooves patterned on one wall, which is similar to the geometry used by Stroock et al. [6]. The off centre position of the apex of the herringbone groove defines its asymmetry. The location of the apex of the groove is positioned at distance *PW* from the wall for a group of 10 grooves (half cycle), where *W* is the width of the channel. The mixer is composed of 5 mixing cycles with 20 grooves in each cycle.

2.2 Test cases

Two cases of optimization are considered:

- **Case–I:** Two design variables, namely, the angle of groove, θ, and the ratio of groove depth to channel height, *d/h* are selected for optimization, while the other variables of the geometry

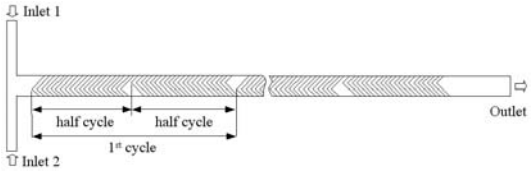

(a)

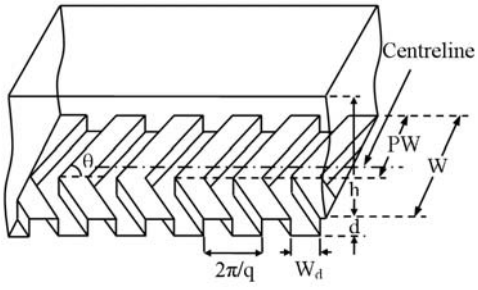

(b)

Fig. 1. Geometry of micromixer with staggered herringbone grooves.

are fixed. Full factorial design is used to select the 9 design points in the deign space.

- **Case-II:** Three design variables namely, ratio of groove width to groove pitch, W_d/Pi, angle of groove, θ and the ratio of groove depth to channel height, d/h, are selected. Fractional factorial D optimal design is used to select the 25 design points in the deign space.

2.3 Numerical analysis

For the numerical analysis of mixing and flow field of the staggered herringbone micromixer, the commercial CFD-code ANSYS CFX-10.0, [13] was used. This is a general purpose code that solves the Navier-Stokes equations using the finite volume method via a coupled solver.

An unstructured tetrahedral grid system shown in Fig. 2 is used with a hexahedral grid at the wall region to capture the velocity gradient near walls. A high quality mesh is critical to achieve accurate results, especially for analysis of the mixing of fluids. The quality of the mesh is examined and modified to speed up convergence and to obtain accurate simulations.

The flow condition in microdevices is purely laminar. Navier-Stokes equations in combination with an advection-diffusion model are applied to analyze the actual mixing phenomena in the microchannel. Water and ethanol are selected as the two operating fluids for mixing.

The velocity at the inlet and zero static pressure at the outlet are specified as boundary conditions. Inlet 1 is assigned 100% ethanol and Inlet 2 100% water. No slip condition is applied at the walls. The properties of water and ethanol at 20 ^{o}C are listed in Table 1. The diffusion coefficient for both water and ethanol is 1.2 x 10^{-9} m^2s^{-1}. The Peclet number (Pe) for the present case is 2.0 x 10^3. The length of the micromixer domain with patterned grooves on the bottom wall for calculation is set at 10mm, since the length for complete mixing is not known.

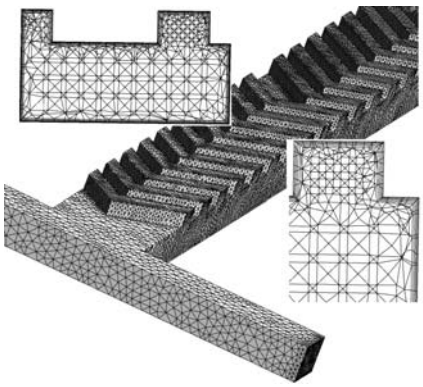

Fig. 2. Example of tetrahedral grid system (θ=45, d/h=0.40 and W_d/Pi=0.50).

2.4 Objective functions and design variables

Quantification of mixing is accomplished by calculating the variance of the species in the micromixer. The variance is based on the concept of the intensity of segregation concept, which is based on the variance of the concentration with the mean concentration. To evaluate the degree of mixing in the micromixer, the variance of the mass fraction of the mixture on a cross-section normal to the flow direction is defined as

$$\sigma_m = \sqrt{\frac{1}{N}\sum (c_i - \bar{c}_m)^2} \tag{1}$$

where N is the number of sampling points inside the cross-sectional area, c_i is the mass fraction at sampling point i, and $\bar{c}_m$ the optimal mixing mass fraction. The number of sampling points is 300, and these sampling points are equidistant on the cross-sectional plane. The values at the sampling points are obtained by interpolations with the values at computational grids. The mixing index M of the fluids at the end of the patterned groove is selected as the objective function as follows:

$$F = [M]_{x=x_o} = \left[1 - \sqrt{\frac{\sigma_m^2}{\sigma_{\max}^2}}\right]_{x=x_o} \tag{2}$$

where σ_{max} is the maximum variance over the data range. The variance is maximum for the completely unmixed fluids, and minimum for completely mixed fluids. The mixing index, M is a normalized parame ter used to evaluate the degree of the mixing of the

Table 1. Properties of fluids at 20 ^{o}C.

Fluid	Density (kg m^{-3})	Viscosity (Kg m^{-1} s^{-1})	Diffusivity (m^2 s^{-1})
Water	9.998 x 10^3	0.9 x 10^{-3}	1.2 x 10^{-9}
Ethanol	7.890 x 10^3	1.2 x 10^{-3}	1.2 x 10^{-9}

fluids. The objective function is calculated on a plane perpendicular to the flow direction at a distance of 10 mm ($x=x_o$), i.e., the end of the patterned groove.

As shown in Fig. 1, there are seven geometric variables: *P, W, h, d, W_d, q,* and *θ.* From these variables, the ratio of groove depth to channel height *d/h* and the angle of grooves θ are selected as the design variables for the Case-1 of optimization. The other variables are fixed as given in Stroock et al. [6]: *h*=77 μm, *W*=200 μm, q= 2л/100 μm^{-1}, W_d= 50 μm, and the groove has asymmetry of *PW* where *P*=2/3. In Case-II, these two variables and ratio of groove width to groove pitch, W_d/Pi are selected as the design variables with *h*=77 μm, *W*=200 μm, q= 2л/100 μm^{-1}, and *P*=2/3.

3. Optimization methodology

The optimization procedure is described in the flowchart shown in Fig. 3. Initially, the variables are selected, and the design space is decided for improvement of system performance. Using design of experiment (DOE), the design points are selected, and at these design points the objective functions are calculated by using flow solver. In this work, the DOE is conducted by using a three-level fractional factorial design. The D-optimal method (Myers and Montgomery, [15]) is used to select the number of design points for the case with three design variables. Evaluations of the objective functions at these design points are carried out by three-dimensional Navier-Stokes analysis.

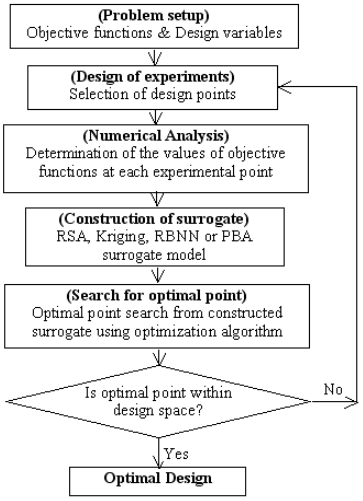

Fig. 3. Optimization procedure.

The next steps are to construct the surrogates and to find optimal points. The surrogate methods used in this work are described below.

3.1 Response surface approximation (RSA) model

In the response surface approximation (RSA) method (Myers and Montgomery, [15]), the following polynomial function is fitted to get the response surface approximation. If the regression coefficients are β's, the polynomial function becomes

$$\hat{F} = \beta_0 + \sum_{j=1}^{n} \beta_j x_j + \sum_{j=1}^{n} \beta_{jj} x_j^2 + \sum \sum_{i \neq j}^{n} \beta_{ij} x_i x_j \quad (3)$$

where n, is number of design variables, and x's are the design variables.

3.2 Radial basis neural network (RBNN) model

The radial basis neural network [16] is two-layered networks with a hidden layer of radial basis transfer function with linear output. The hidden layer consists of a set of radial basis functions that act as activation functions, the response of which varies with the distance between the input and the centre. The distance between two points is determined by the difference of their coordinates and by a set of parameters. The main advantage of using the radial basis approach is the ability to reduce the computational cost due to the linear nature of the radial basis functions. The linear model *f* for the function can be expressed as a linear combination of a set of *N* basis functions,

$$f(x) = \sum_{j=1}^{N} w_j y_j \quad (4)$$

where w_j is weight and y_j is basis function. There are several possibilities for the choice of basis functions. If the basis function and other parameters are fixed through the training process, the model is linear. However, if the basis function changes during the training/learning process the model is non-linear. The learning process is equivalent to finding a surface in multidimensional space that provides a best fit to the training data which is further used to interpolate the test data. The parameters for fitting this surrogate model are spread constant (SC) and a user-defined error goal (EG). The allowable error goal is decided from the allowable error from the mean input re-

sponses. In the present study, we used customized RBNN function, *newrb* available in (MATLAB, [14]).

3.3 Kriging (KRG) model

Kriging model (Martin and Simpson, [17]) is an interpolating meta-modeling technique that employs a trend model f(x) to capture large-scale variations and a systematic departure Z(x) to capture small scale variations. Kriging postulation is the combination of global model and departures of the following form:

$$\hat{F}(x) = f(x) + Z(x) \tag{5}$$

where $\hat{F}(x)$ represents the unknown function, f(x) is global model, while Z(x) represents the localized deviations. Z(x) is the realization of a stochastic process with mean zero and non-zero covariance. A linear polynomial function is used as trend model and the systematic departure terms follow Gaussian correlation function.

3.4 PRESS based averaging (PBA) model

A weighted average model proposed by Goel et al. [4] is adopted in the present investigation. It is based on the PRESS-based-averaging (PBA) model (termed WTA3 by Goel et al. [5]. The predicted response is defined as follows for the PBA model:

$$\hat{F}_{wt.avg}(x) = \sum_{i}^{N_{SM}} w_i(x)\,\hat{F}_i(x) \tag{6}$$

where, N_{SM} is the number of basic surrogate models used to construct weighted average model, i^{th} surrogate model at design point x produces weight $w_i(x)$ and $\hat{F}_i(x)$ is the predicted response by i^{th} surrogate model.

Weights are decided by using the guideline that the weights should reflect our confidence in the surrogate model such that the surrogate which produces high error has low weight, and thus low contribution to the final weighted average surrogate, and vice-versa. In this work, global weights are selection by using generalized mean square cross-validation error (GMSE) or PRESS (in RSA terminology) that is a global data-based measure of goodness. The generalized mean square cross-validation error calculation procedure is given in the appendix.

The weighting scheme used in PRESS-based averaging surrogate is given as follows:

$$w_i^* = \left(E_i \Big/ E_{avg} + \alpha \right)^{\beta}, \qquad w_i = w_i^* \Big/ \sum_i w_i^*$$
$$E_{avg} = \sum_{i=1}^{N_{SM}} E_i \Big/ N_{SM}; \qquad \beta < 0, \alpha < 1 \tag{7}$$
$$E_i = \sqrt{GMSE_i}, i = 1, 2, \ldots, N_{SM}$$

Two constants α and β are chosen as α=0.05 and β=-1.0 , (Goel et al., [4]).

Next, RSA, Kriging, RBNN and PBA surrogate models are constructed from objective function values at design points. Eqs. (6) and (7) are used to construct the weighted average surrogate model. The constructed surrogates are used to search for optimal points by using sequential quadratic programming (SQP) (function, fmincon in (MATLAB, [14]).

4. Results and discussion

The present shape optimization is performed for a micromixer geometry with patterned herringbone grooves on a single wall, as shown in Fig. 1, for Pe=2.0 x10^3 with water and ethanol as the two working fluids. In a previous work (Ansari and Kim [12]) where the same analysis methods were used, the computational results were qualitatively compared with the experimental results of Stroock et al. [6] for the distribution of variance, σ_M, in Fig. 4. The fluids considered in their experimental analysis were water and a solution of 80% glycerol and 20% water. The viscosity of the glycerol/water solution is 67.0 g $m^{-1}s^{-1}$, while that of ethanol is 1.2 $gm^{-1}s^{-1}$. However, the pre-

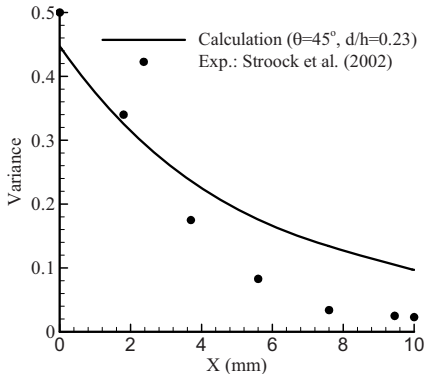

Fig. 4. Validation of numerical results (Ansari and Kim, [12]).

sent numerical calculation and optimization are per formed with water and pure ethanol for Pe =2.0 x10^3. The mixer for the experiment of Stroock et al. [6] with 15 cycles of patterned grooves is much longer than that considered in this work. Thus, the discrepancy shown in Fig. 4 is due to these differences in geometry and working fluids. However, the qualitative trend of the computational results is quite similar to the experimental findings.

Different surrogate models are applied to optimize the groove shape in order to compare the results predicted by these surrogate models. Two cases of optimization with single objective function are considered. Ranges of design variables for the two cases are shown in Table 2.

4.1 Case –I

The herringbone groove of the micromixer is optimized with two design variables, namely the ratio of depth of groove to channel height, *d/h* and the angle of groove, θ. Results of optimization are shown in Tables 3 and 4. Table 3(a) shows errors (E_{cv}) obtained from the cross validation and weights for the surrogates. The values of the weights are used to construct the PBA model. RSA produces the least E_{cv} value, 1.12 x 10^{-2} while RBNN gives the highest E_{cv} value, 6.45 x 10^{-2}. Hence, these two surrogate models, RBNN and RSA, are assigned weights in inverse order of the magnitude of E_{cv} as, 0.127 and 0.649, respectively to construct the PBA model.

Table 3(b) shows values of the design variables and the objective function ($F_{surrogate}$) predicted by the various surrogates at the optimal points. The values of the objective function (F_{NS}) computed by Navier-Stokes (NS) equations at the optimal points are also shown. It is clear from the table that all the surrogate models predict values of the objective function higher than those for the reference geometry (θ=45.0, W_d/Pi=0.50 and *d/h*=0.23) Stroock et al. [6]. The highest improvement in the objective function, 9.24% is achieved by the RSA model while the RBNN model predicts the least 7.83% in comparison with the reference geometry. Comparison of predicted values by the surrogate models with corresponding calculated values by NS analysis shows the lowest error, 0.02% for RSA model and the highest error, 4.14% for RBNN model. Thus, RSA gives the highest objective function value (F_{NS}), i.e., the main goal of the optimization, as well as the best accuracy in predicting the objective function at the optimal point. The performance of the multiple surrogate model, PBA, is medium both in the improvement of objective function and in its accuracy in prediction, which means that the PBA model neither produces the best result nor the worst.

Table 3(c) shows the predictions of objective function ($F_{surrogate}$) by each surrogate at all of the optimal points. Each shaded cell shows the value of the objective function at the optimal point predicted by itself. For example, predicted objective function values at PBA generated optimal point are 0.8796, 0.8777, 0.8791 and 0.8757 by PBA, RBNN, RSA and KRG models, respectively. Fig. 5 shows the absolute errors ($|F_{NS} - F_{surrogate}|$) in predictions of each surrogate

Table 2. Design variables and ranges.

	Variables	Lower Limits	Upper Limits
CASE-I	θ (degree)	45	70
	d/h	0.23	0.50
CASE-II	W_d/Pi	0.40	0.60
	θ (degree)	45	70
	d/h	0.23	0.50

Table 3(a). Weights for weighted average model (PBA) for *F* in Case-I.

MODEL	Cross Validation Error, E_{cv}	Weight
RBNN	6.45x10^{-2}	0.127
RSA	1.12x10^{-2}	0.649
KRG	3.61x10^{-2}	0.223

Table 3(b). Optimal designs suggested by various surrogates (Case-I).

Optimal design variables		Surrogates			
		PBA	RBNN	RSA	KRG
θ		53.01	53.34	53.18	56.77
d/h		0.4657	0.4312	0.4842	0.50
Objective function statistics	$F_{surrogate}$	0.8796	0.9052	0.8808	0.8715
	F_{NS}	0.8724	0.8692	0.8806	0.8729
	F_{NS} - $F_{surrogate}$	-0.83 x10^{-2}	-3.60 x10^{-2}	-0.02 x10^{-2}	-0.14 x10^{-2}
		-0.95%	-4.14%	-0.02%	-0.16%
	$F_{reference}(NS)$	0.8061			
	$F_{reference}$ - F_{NS}	-6.63 x10^{-2}	-6.31 x10^{-2}	-7.45 x10^{-2}	-6.68 x10^{-2}
		8.22%	7.83%	9.24%	8.29%

Table 3(c). Predictions by surrogate models at each optimal point (Case-I).

Objective function values predicted by	Optimal points predicted by			
	PBA	RBNN	RSA	KRG
PBA	0.8796	0.8993	0.8803	0.8662
RBNN	0.8777	0.9051	0.8768	0.8646
RSA	0.8791	0.8909	0.8808	0.8677
KRG	0.8757	0.8675	0.8788	0.8714
NS analysis	0.8724	0.8692	0.8806	0.8729

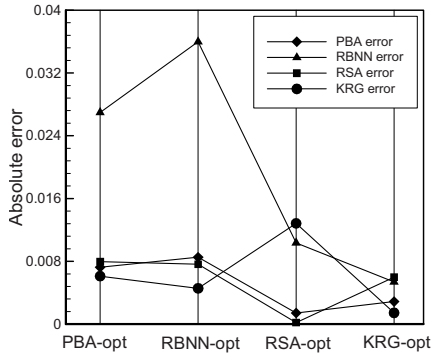

Fig. 5. Absolute errors, $|F_{NS} - F_{surrogate}|$ in prediction by different surrogates at optimal points (case-I).

model at all of the optimal points. KRG predicts the least errors at all optimal points except the optimal point generated by RSA. RBNN produces the highest error at its own optimal point while RSA and KRG produce the least errors at their own optimal points, respectively.

4.2 Case-II

In this case, the micromixer is optimized with three design variables, i.e., the ratio of depth of groove to channel height, *d/h*, the angle of groove, θ, and ratio of groove width to groove pitch, W_d/Pi. Table 4(a) shows errors (E_{cv}) obtained from the cross validation and weights for the surrogates in the PBA model. Unlike Case-I, RBNN produces the least E_{cv} value, 1.39×10^{-2} while RSA gives the highest E_{cv} value, 2.15×10^{-2}. Hence, these two surrogate models, RBNN and RSA, are assigned weights as 0.402 and 0.265, respectively, to construct the PBA model.

Table 4(b) shows the values of design variables and the objective function predicted by the various surrogates at the optimal points as well as the objective function values computed by NS equations at the optimal points. The highest improvement in the objective function, 9.18%, is achieved by the RBNN model while the KRG model predicts the least, 8.31%, in comparison with the reference shape (Stroock et al. [8]). $F_{surrogate}$-F_{NS} at each optimal point shows the highest error, 2.02%, for the RSA model and the lowest error, 0.11%, for the KRG model. Thus, KRG shows the best accuracy at the optimal point, but the highest value of optimal objective function (F_{NS}) is obtained by RBNN. As also shown in Case-I, the PBA model neither produces the best result nor the worst.

Table 4(a). Weights for weighted average model (PBA) for *F* in Case-II.

MODEL	Cross Validation Error, E_{cv}	Weight
RBNN	1.39×10^{-2}	0.402
RSA	2.15×10^{-2}	0.265
KRG	1.71×10^{-2}	0.332

Table 4(b). Optimal designs suggested by various surrogates (Case-II).

Optimal design variables		Surrogates			
		PBA	RBNN	RSA	KRG
W_d/Pi		0.5457	0.5575	0.5485	0.5344
θ		51.36	49.92	50.60	59.70
d/h		0.4513	0.4465	0.4515	0.4664
Objective function statistics	$F_{surrogate}$	0.8881	0.8976	0.8969	0.8741
	F_{NS}	0.8781	0.8801	0.8791	0.8731
	$F_{NS} - F_{surrogate}$	-1.00×10^{-2}	-1.75×10^{-2}	-1.78×10^{-2}	-0.10×10^{-2}
		-1.14%	-1.91%	-2.02%	-0.11%
	$F_{reference}$(NS)	0.8061			
	$F_{reference} - F_{NS}$	-7.2×10^{-2}	-7.4×10^{-2}	-7.3×10^{-2}	-6.7×10^{-2}
		8.93%	9.18%	9.05%	8.31%

It is noted that the highest improvement in the objective function is reduced from 9.24% by RSA in Case-I to 9.18% by RBNN in Case-II even though an additional design variable is employed in Case-II. However, by increasing the number of design variables, all of the predicted values ($F_{surrogate}$) at the optimal points are improved, and the corresponding values of $F_{NS,}$ except for RSA, are also improved. RSA shows the highest prediction of objective function in Case-II, but due to large deterioration of the accuracy (from -0.02% to -2.02%) at the optimal point, the highest improvement in objective function is reduced compared to Case-I.

Table 4(c) shows the predictions at all of the optimal points by the surrogates. Fig. 6 shows the absolute errors ($|F_{NS} - F_{surrogate}|$) in predictions of each

Table 4(c). Predictions by surrogate models at each optimal point (Case-II).

Objective function values predicted by	Optimal points predicted by			
	PBA	RBNN	RSA	KRG
PBA	0.8881	0.8967	0.8979	0.8697
RBNN	0.8875	0.8976	0.8958	0.8685
RSA	0.8862	0.8929	0.8992	0.8676
KRG	0.8812	0.8836	0.8865	0.8741
NS analysis	0.8781	0.8801	0.8791	0.8731

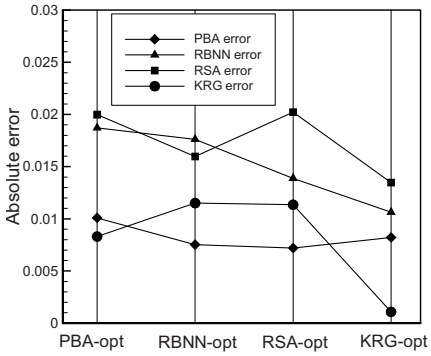

Fig. 6. Absolute errors, $|F_{NS} - F_{surrogate}|$ in prediction by different surrogates at optimal points (case-II).

surrogate at all of the optimal points. PBA shows the least errors at the optimal points generated by RBNN and RSA, while KRG shows the least errors at the optimal points generated by PBA and KRG. The trend of error by PBA is quite uniform as compared to other surrogates in both Case-I and Case-II (Figs. 5 and 6). And, it is noted that KRG shows the least error at its own optimal point in both cases.

The root mean square (RMS) errors calculated from Figs. 5 and 6 are presented in Fig. 7. The PBA model shows the lowest RMS error in both cases. Both PBA and KRG models show relatively smaller errors consistently in both cases. But, RBNN and RSA models show large variations in the error depending on the case.

In the application of surrogate models to turbomachinery blade optimization, Samad et al. [18] reported that the most accurate surrogate is the RSA model for the three different objective functions tested. The RBNN model predicts the optimal points where the NS computed objective function values show the best results for two objective functions and RSA produced the best result for one objective function. However, the KRG model shows the worst performance in all cases. The PBA model shows moder-

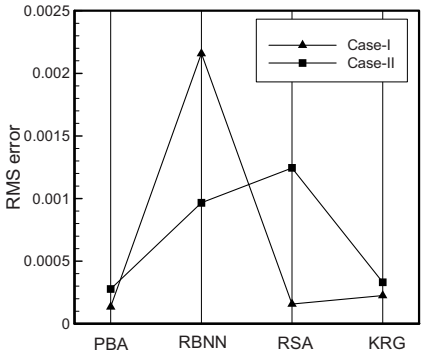

Fig. 7. RMS errors produced by the surrogates.

ate performance. The RSA model, which shows the best overall performance in a turbomachinery application, shows also the best performance in Case-I, but does not show such performance in Case-II in this application to micromixer optimizations. This reflects the strong problem-dependent nature of the surrogate models.

The multiple surrogate model, PBA, does not predict the best optimal point, but the result predicted is also not worst in all cases. And, this model shows the best reliability in predicting the objective function values in design space. The beauty of the PBA model is that it protects the designers from predicting badly from poor performing surrogates, since this model is based on the global data based error and the contribution of the worst performing surrogate is the least to construct this surrogate.

5. Conclusion

Performances of surrogate models have been compared for the optimizations of a herringbone grooved micromixer. The mixing index at the exit has been selected as the single objective function. All surrogates models give significant improvements in the mixing index in comparison with the reference geometry. Among the surrogates, the RSA model shows the best overall performance in the case with two design variables, but for three design variables the RBNN predicts the highest objective function, while the KRG shows the best accuracy at the optimal point. This reflects the strong problem-dependent nature of the surrogate models. Even though the weighted surrogate model, PBA, is not the best in any case, it gives quite reliable and consistent results in most cases. Hence, the use of the PBA model protects de-

signer against choosing a poor surrogate. Therefore, the application of PBA model enhances the robustness of the optimization process.

Acknowledgments

This work was supported by the Korea Science & Engineering Foundation (KOSEF) grant funded by the Korea government (MOST) (No. R01-2006-000-10039-0).

Nomenclature

D	:	Diffusivity of the fluid
F	:	Objective function
L	:	Length of the channel
Pi	:	Groove pitch
M	:	Mixing index
P	:	Asymmetry of the groove
Pe	:	Peclet number
R^2_{adj}	:	Adjusted R square
Re	:	Reynolds number
W	:	Channel width
W_d	:	Groove width
d	:	Depth of groove
h	:	Channel height
p	:	Pressure in channel
Δp	:	Pressure drop
q	:	Wave vector of ridges
x,y,z	:	Streamwise, spanwise, and cross-streamwise coordinates

Greek symbols

α, β	:	Exponents for weighted average models
σ	:	Variance
μ	:	Absolute viscosity of fluid
θ	:	Angle of the groove
ρ	:	Fluid density

Subscripts

m	:	Mixture
opt	:	Optimum value
NS	:	Navier-Stokes
d	:	Ditch/groove
i	:	Sampling point
max	:	Maximum value
x	:	Axial distance

References

[1] N. V. Queipo, R. T. Haftka, W. Shyy, T. Goel, R. Vaidyanathan and P. K. Tucker, Surrogate-based analysis and optimization, *Prog. in Aerospace. Sci.* 41 (2005) 1-28.

[2] W. Li and S. Padula, Approximation methods for conceptual design of complex systems, Eleventh International Conference on Approximation Theory (eds. C. Chui, M. Neaumtu, L. Schumaker) (2004) 241-278.

[3] L. Zerpa, N. V. Queipo, S. Pintos and J. Salager, An optimization methodology of alkaline-surfactant-polymer flooding processes using field scale numerical simulation and multiple surrogates, *J. of Petroleum Sci. and Eng.* 47 (2005) 197-208.

[4] T. Goel, R. Haftka, W. Shyy and N. Queipo, Ensemble of surrogates, *Struct. and Multidisciplinary Optimization*, 33 (3) (2007) 199-216.

[5] T. Goel, J. Zhao, S. Thakur, R. T. Haftka and W. Shyy, Surrogate model-based strategy for cryogenic cavitation model validation and sensitivity evaluation, 42nd AIAA/ASME/ SAE/ASEE Joint Propulsion Conference and Exhibit, Sacramento, USA. AIAA (2006) 2006-5047.

[6] A. D. Stroock, S. K. W. Dertinger, A. Ajdari, I. Mezic, H. A. Stone and G. M. Whitesides, Chaotic mixer for microchannels. *Science* 295 (2002) 647-651.

[7] V. Hessel, H. Lowe and F. Schonfeld, 2005, Micromixers-a review on passive and active mixing principles. *Chem. Eng. Sci.* 60 (2005) 2479-2501.

[8] A. D. Stroock and G. J. McGraw, Investigation of the staggered herringbone mixer with a simple analytical model. *Philos. Trans. R. Soc. London, Ser. A,* 362 (2004) 971-986.

[9] J. Aubin, D. F. Fletcher, J. Bertrand and C. Xuereb, Characterization of the mixing quality in micromixers. *Chem. Eng. Tech.* 26 (12) (2003) 1262-1270.

[10] D. G. Hassel and W. B. Zimmerman, Investigation of the convective motion through a staggered herringbone micromixer at low Reynolds number flow. *Chem. Eng. Sci.* 61 (2006) 2977-2985.

[11] G. N. Vanderplaats, Numerical optimization techniques for engineering design with applications, McGraw-Hill, 1984.

[12] M. A. Ansari and K. Y. Kim, Application of radial basis neural network to optimization of a micromixer. *Chem. Eng. Tech.* 30 (7) (2007) 962–966.

[13] CFX-10.0, Solver Theory, ANSYS 2004.

[14] MATLAB®, The language of technical computing, Release 14, The MathWorks Inc.

[15] R. H. Myers and D. C. Montgomery, Response surface methodology: process and product optimization using designed experiment, Wiley, New York, (1995).
[16] M. L. J. Orr, Centre for Cognitive Science, Edinburgh University, EH 9LW, Scotland, UK, (http://anc.ed.ac.uk/rbf/rbf.html), (1996).
[17] J. D. Martin and T. W. Simpson, Use of kriging models to approximate deterministic computer models. *AIAA Journal* 43 (4) (2005) 853-863.
[18] A. Samad, K. Y. Kim, T. Goel, R. T. Haftka and W. Shyy, Shape optimization of turbomachinery blade using multiple surrogate models, 10th International Symposium on Advances in Numerical Modeling of Aerodynamics and Hydrodynamics in Turbomachinery, ASME Joint-U.S.-European Fluids Engineering Summer Meeting, Miami, FL, USA, FEDSM2006-98368.

Appendix

Generalized mean square cross-validation error (GMSE)

The gross mean square cross validation error is calculated to get the weights for weighted average methods. In general, the data is divided into k subsets (k-fold cross-validation) of approximately equal size. A surrogate model is constructed k times, each time leaving out one of the subsets from training, and using the omitted subset to compute the error measure of interest. The generalization error estimate is computed by using the k error measures obtained (e.g., average). If k equals the sample size, this approach is called leave-one-out cross-validation (also known as PRESS in the polynomial response surface approximation terminology). Following equation represents a leave-one-out calculation when the generalization error is described by the mean square error (GMSE).

$$GMSE = \frac{1}{k}\sum_{i=1}^{k}(f_i - \hat{f}_i^{(-i)})^2$$

where, $\hat{f}_i^{(-i)}$ represents the prediction at $\mathbf{x}^{(i)}$ using the surrogate constructed with all sample points except ($\mathbf{x}^{(i)}$, f_i).